Available online at www.sciencedirect.com
SCIENCE DIRECT®
International Journal of Pharmaceutics 295 (2005) 247–260
international journal of pharmaceutics
www.elsevier.com/locate/ijpharm

Pharmaceutical Nanotechnology

Cationic albumin conjugated pegylated nanoparticle with its transcytosis ability and little toxicity against blood–brain barrier

Wei Lu [a], Yu-Zhen Tan [b], Kai-Li Hu [a], Xin-Guo Jiang [a,*]

[a] *Department of Pharmaceutics, School of Pharmacy, Fudan University, P.O. Box 130, Shanghai 200032, China*
[b] *Department of Anatomy and Histology and Embryology, Shanghai Medical School, Fudan University, Shanghai 200032, China*

Received 7 December 2004; received in revised form 28 January 2005; accepted 30 January 2005
Available online 1 April 2005

Abstract

Our newly developed drug delivery carrier, cationic bovine serum albumin (CBSA) conjugated with poly(ethyleneglycol)-poly(lactide) (PEG-PLA) nanoparticle (CBSA-NP), was designed for brain drug delivery. CBSA, as a brain specific targetor, was covalently conjugated with the maleimide function group at the distal of poly(ethyleneglycol) (PEG) surrounding the nanoparticles. To evaluate its blood–brain barrier (BBB) transcytosis and toxicity against the BBB endothelial tight junction, we have explored a method of coculture with brain capillary endothelial cells (BCECs) on the top of micro-porous membrane of cell culture insert and astrocytes on the bottom side. The permeability of ^{14}C-labeled sucrose was determined. For the CBSA-NP transcytosis study, a lipophilic fluorescent probe, 6-coumarin, was incorporated into nanoparticles. The BBB permeability of CBSA-NP in vitro was calculated and compared with native bovine serum albumin (BSA) conjugated pegylated nanoparticles (BSA-NP). As the coculture model, the transendothelial electrical resistance reached up to $313 \pm 23\,\Omega\,cm^2$. The tight junction between BCECs in the coculture could be visualized by scanning electron microscopy and transmission electron microscopy. The unchanged permeability of ^{14}C-labeled sucrose comparing to that in the appearance of 200 μg/ml of CBSA-NP proved that CBSA-NP did not impact the integrity of BBB endothelial tight junctions. CBSA-NP also showed little toxicity against BCECs. The permeability of CBSA-NP was about 7.76 times higher than that of BSA-NP, while the transcytosis was inhibited in the excess of free CBSA. It was concluded that CBSA-NP preferentially transported across BBB with little toxicity, which offered the possibility to deliver therapeutic agents to CNS.

Keywords: Blood–brain barrier (BBB); Coculture; Cationic bovine serum albumin (CBSA); Pegylated nanoparticle; Transcytosis; Toxicity

1. Introduction

Blood–brain barrier (BBB) is composed of specific structures by brain capillary endothelial cells and

* Corresponding author. Tel.: +86 21 5423 7381; fax: +86 21 5423 7381.
E-mail address: xgjiang@shmu.edu.cn (X.-G. Jiang).

0378-5173/$ – see front matter © 2005 Elsevier B.V. All rights reserved.
doi:10.1016/j.ijpharm.2005.01.043

its sheathing by astrocytic endfeet through basement membrane, which maintains homeostasis of central nerve system (CNS) by its specific properties. The distinct anatomical feature of BBB is characterized as endothelial tight junctions, minimal endothelial pinocytosis, and full investment of the abluminal side of the capillary endothelium by astrocyte foot processes. BBB protects the brain from the blood milieu, selectively transports various nutriens and effluxes the noxious and metabolites, metabolizes and modifies blood or brain borne substances. Nevertheless, this self-protection mechanism can hinder drugs to penetrate into the CNS. Approximately 100% of large molecule drugs do not cross BBB. Greater than 98% of small-molecule drugs do not cross BBB (Pardridge, 2003). Therefore, the issue of CNS delivery of candidate drugs must be placed more emphasis on with BBB drug targeting technology.

The immunoliposomes or immunonanoparticles which the brain specific targetors were covalently conjugated to polyethyleneglycol (PEG) modified liposomes (pegylated liposomes) or nanoparticles (pegylated nanoparticles) as drug carrier via the tips of its functional PEG strands, proved successful in brain drug delivery. Pardridge developed mouse monoclonal antibody against the rat transferrin receptor, OX26, coupled with pegylated liposome to deliver drug into CNS (Huwyler et al., 1996). This immunoliposome succeeded in delivery of small molecules such as daunomycin (Huwyler et al., 1996) and plasmid DNA (Shi and Pardridge, 2000; Shi et al., 2001; Zhang et al., 2003, 2004). The OX26 conjugated pegylated nanoparticles were also synthesized (Olivier et al., 2002). In addition, cationic bovine serum albumin (CBSA) coupled pegylated liposomes were taken up into brain endothelium via an absorptive mediated endocytotic pathway and proved to be a suitable carrier for brain drug delivery under the confocal laser scanning fluorescence microscopy (Thöle et al., 2002). The advantages of immunoliposomes and immunonanoparticles are of the specific brain delivery property, larger drug loading capacity, disguise of limiting characteristics of drugs with physical nature of the liposome or nanoparticles and reduction of drug degradation in vivo. The surface modification of PEG enables the liposomes or nanoparticles to escape the arrest of mononuclear phagocytic system (MPS) so as to prolong its half-life in plasma and increase the area under the concentration–time curve (AUC) (Bazile et al., 1995).

In this principle, we have developed CBSA conjugated pegylated nanoparticles (CBSA-NP) as a novel drug carrier for brain delivery. We used a bifunctional PEG, maleimide-polyethyleneglycol (maleimide-PEG), containing a maleimide group at one terminus and free hydroxyl group at the other terminus to initiate maleimide-polyethyleneglycol-poly(lactide) (maleimide-PEG-PLA). The pegylated nanoparticles were prepared by the mixture of this novel copolymer and methoxypolyethyleneglycol-poly(lactide) (MPEG-PLA) copolymer using emulsion/solvent evaporation technique. The molecular weight of PEG in maleimide-PEG was chosen higher than that in methoxypolyethyleneglycol (MPEG), so that the maleimide function would protrude from the MPEG corona to be available for conjugating the thiolated CBSA under the mild condition to form CBSA-NP. CBSA at the surface of the nanoparticles with pI of 8–9, was shown as a favorable brain targetor with a longer serum half-life and a greater degree of selectivity to brain tissue as compared to other organs (liver, heart, lung), which may facilitate the absorptive mediated transcytosis (AMT) (Bickel et al., 2001).

In order to investigate the transcytosis ability of CBSA-NP and whether it was toxic to the integral of BBB tight junction or not, we developed a coculture model of rat blood–brain barrier in vitro. The rat brain capillary endothelial cells (BCECs) and astrocytes were both isolated from newborn rats. The coculture was performed with BCECs on the top side of cell culture insert membrane and astrocytes on the bottom side, which allowed the astrocytes to spread their processes through the microporous membrane so as to contact the BCECs. This “contact through feet” model proved to closely mimic BBB specific situation in vivo through its morphological and functional characterization with scanning electron microscopy (SEM), transmission electron microscopy (TEM) and transendothelial electric resistance (TEER) measurement. For the CBSA-NP transcytosis study, a lipophilic fluorescent probe with high sensitivity, 6-coumarin, was incorporated into nanoparticles, and the BBB permeability of CBSA-NP in vitro was detected with high performance liquid chromatography (HPLC)-fluorescence detection method, compared with native

bovine serum albumin (BSA) conjugated pegylated nanoparticles (BSA-NP). The permeability of ^{14}C-labeled sucrose coadministered with CBSA-NP in the coculture model was calculated to clarify whether this novel drug carrier had the toxicity to open the tight junctions.

2. Materials and methods

2.1. Materials and animals

The copolymers of methoxy-PEG-PLA and maleimide-PEG-PLA were synthesized by ring opening polymerization of D,L-lactide (99.5% pure, PURAC) initiated by MPEG (MW 3000 D, SUNBRIGHT^{TM} MEH-30H, NOF Corporation, Lot No. 14530, Japan) and maleimide-PEG (MW 3400 D, NEKTAR^{TM}, Lot No. PT-08D-16, Huntsville, AL, USA), respectively, in the appearance of stannous octate in our laboratory. Bovine serum albumin V (BP0042 Roche) and calf serum (CS) were purchased from Huamei Bioengineering Company (China); 6-coumarin, from Aldrich; dextran (MW $\sim$ 100 kD), from Fluka Chemie GmbH (Riedel-de Haën Brand, Germany); 1-ethyl-3-(dimethylaminopropyl)-carbodiimid-hydrochloride (EDAC) and 5,5′-dithiobis(2-nitrobenzoic acid) (Ellmann's reagent), from Acros (Belgium); endothelial cell growth supplement (ECGS), basic fibroblast growth factor (bFGF), Megacell® DMEM (high glucose) cell culture medium, collagenase type II and gelatin, from Sigma company (St Louis, USA); plastic cell culture dishes, plates and flasks, from Corning Incorporation (New Jersey, USA); fetal bovine serum (FBS), from Gibco (USA); 12-well Falcon^{TM} Cell culture insert with poly-(ethylene terephtalate) (PET) membranes (pore size was 1.0 μm, pore density was 1.6×10^6 pores/cm^2), from Becton Dickinson Company (Franklin Lakes, USA); U-^{14}C-labeled sucrose (643 mCi/mmol), from Amersham Biosciences (Buckinghamshire, UK). Double distilled water was purified using a Millipore Simplicity System (Millipore, Bedford, USA). All the other chemicals were analytical reagent grades and used without further purification.

The animals used for the experiment were treated according to protocols evaluated and approved by the ethical committee of Fudan University.

2.2. Preparation and characterization of CBSA-NP and BSA-NP

The pegylated nanoparticles (NPs) made of a blend of MPEG-PLA and maleimide-PEG-PLA were prepared through the emulsion/solvent evaporation technique (Olivier et al., 2002). The preparation of nanoparticles loaded with 6-coumarin was the same as that of blank NPs, except that 15 μl 6-coumarin (1 mg/ml stock solution in dichloromethane) was additionally added to dichloromethane solution containing copolymers before primary emulsification.

CBSA was prepared from BSA by cationization with ethylenediamine in the appearance of EDAC (Thöle et al., 2002). Isoelectric focusing (IEF) of CBSA showed that the pI of CBSA had a shift from 4 to 8–9, and SDS-PAGE depicted that the molecular weight of CBSA did not change in comparison with that of BSA, i.e. approximately 66 kD. CBSA was then thiolated using 2-iminothiolane (Traut's reagent) (Huwyler et al., 1996). Ellman's reagent was used to determine the extent of thiolation (Ellmann, 1959) with a thiolation degree of an average of about 1.5 mol thio-group per mol CBSA.

The thiolated CBSA was mixed with nanoparticles at a thiolated CBSA:maleimide ratio of 1:1. The volume of mixture was 1 ml, the conjugation of CBSA to the blank or nanoparticles loaded with 6-coumarin was performed overnight on a rotating plate set at a low speed. The reaction mixture was then applied to a 1.6 cm × 20 cm Sepharose CL-4B column and eluted with 0.01 M PBS buffer (pH 7.4). The milky CBSA-NP fractions were visually identified and collected, and the nanoparticle concentration was determined by turbidimetry using UV 2401 spectrophotometer at 350 nm (Shimadzu, Japan). The thiolation of BSA, conjugation to nanoparticle, the mix ratio of thiolated BSA to maleimide and separation of BSA-NP were the same as those of CBSA-NP.

The mean (number based) diameter and zeta potential of the nanoparticles were determined by dynamic light scattering (DLS) using a Zeta Potential/Particle Sizer NICOMPTM 380 ZLS (PSS.NICOMP Particle Size System, Santa Barbara, USA).

CBSA-NP and BSA-NP were dissolved in methanol, and 6-coumarin content was detected by HPLC analysis (Davda and Labhasetwar, 2002). A 20 μl diluted sample was injected in the system (Shi-

madzu Scientific Instrument Inc., Japan) consisting of a pump (LC-10ATVP) and a fluorescence detector (Model RF-10AXL, Ex 465 nm/Em 502 nm). With a Dikma Diamonsil C18 (5 μm, 200 mm × 4.6 mm) column, the separations were achieved in methanol: 20 mM ammonium acetate buffer (93:7, pH 4.0) mobile phase with flow rate of 1.2 ml/min and column temperature of 35 °C. The 6-coumarin loading efficiency (DLE) was calculated by the following equation:

$$\text{DLE\%} = \frac{6 - \text{coumarin concentration in nanoparticle solution}}{\text{nanoparticle concentration in the same solution}} \times 100\%$$

The release test of 6-coumarin in vitro was performed by incubating 1.0 ml about 2 mg of 6-coumarin loaded CBSA-NP in a dialysis bag and immersed in 19.0 ml pH 4 and 7.4 PBS, which represents the endolysosomal compartment and physiologic pH, respectively (Panyam et al., 2003b). The released samples were also analyzed by HPLC method (Panyam et al., 2003b).

2.3. Cell culture

2.3.1. Isolation of rat BCECs and astrocytes

The isolation of BCECs was modified according to previously described techniques (Méresse et al., 1989; Dehouck et al., 1992; Cecchelli et al., 1999; Demeuse et al., 2002). Briefly, the brain cortices of SD rats 1–3 days after birth were dissected free of meninges and minced. The homogenate was digested in 0.05% trypsin at 37 °C for 30 min, followed by 15% dextran (1:1, v/v) density centrifugation at 2000 rpm for 20 min. The pellet was resuspended with HBSS and filtered through a 150 μm mesh sieve. The capillaries were collected on the sieve after a second filtration (75 μm). After 1 mg/ml collagenase type II digestion at 37 °C for 30 min, capillaries were resuspended by 1 ml DMEM containing 20% FBS, penicillin (100 U/ml) and streptomycin (100 mg/ml), and seeded into a 35 mm diameter culture dish coated with 1% gelatin. On the 4th day, ECGS and bFGF were added at the final concentration of 0.2 mg/ml and 10 ng/ml, respectively. The culture medium was changed every three days. On the 10th day, five largest endothelial colonies were retained and the remainder was scraped. Cells were subpassaged until confluency. BCECs used for making coculture and nanoparticle uptake study were passage 3–7.

The isolation procedure of astrocytes from rat brain was modified (McCarthy and De Vellis, 1980). The cortex of brain of SD rats 1–2 days after birth were dissected free of meninges, cut away and minced into 1–2 mm cube, then digested in 0.05% trypsin at 37 °C for 20 min. The tissue was further dispersed into free cells by using pipette in DMEM supplemented 10% CS. After several minutes' free sedimentation of tissue residue, the supernatant was collected. This step was repeated until the tissue was ultimately dispersed. Forced through a 150 μm filter and centrifuged, the collected cells was resuspended in DMEM containing 15% CS, glucose (6 mg/ml), L-glutamine (0.18 mM), penicillin (100 U/ml) and streptomycin (100 mg/ml). After a second filtration (75 μm), the cells were seeded on plastic flask at a density of 1.5×10^6 cells/ml. The medium was changed every 3 days. After 9–10 days, the flasks were shaken at the speed of 260 rpm at 37 °C for 18 h to eliminate the contaminating microglias and oligodendrocytes. Floating cells discarded, the purified astrocytes were refreshed with culture medium, allowed to reach confluency. Astrocytes were then subpassaged at a density of 3×10^4 cells/ml.

2.4. Coculture of BCECs and astrocytes

BCECs and astrocytes were cocultured in a "contact through feet" model (Hayashi et al., 1997; Dehouck et al., 1995; Demeuse et al., 2002). In a 12-well cell culture insert with 1 μm-diameter microporous PET membrane, astrocytes were transferred at second passage on the bottom side at a density of 1.2×10^6 cells/ml by placing the insert upside down. After 4 h, the astrocytes attached firmly, then the membrane was turned over and placed in 12-well culture plate. DMEM supplemented 20% FBS was added and changed every other day. After 4–5 days, BCECs were seeded on the upper side at a concentration of 1.6×10^5 cells per insert. After 10–12 days, TEER was measured (Millicell ERS, Millipore, Bedford, USA) and the coculture was used for experiment.

The coculture sample was fixed at room temperature for 1 h with glutaraldehyde (2.5% v/v) in PBS, then postfixed in osmium tetroxide (1% w/v) at 4 °C for 2 h followed by dehydration in ethanol. After critical point drying, SEM samples were sputtered with

gold (50 nm) in an IB-3 sputtering machine (Japan) and observed in a Hitachi S-520 scanning electron microscope (Japan). TEM samples were embedded in epoxy resin, then ultrathin sections were cut and observed in a Philip CM120 transmission electron microscope.

2.5. BBB permeability studies of ^{14}C-labeled sucrose in vitro

The study of transport was performed according to previous reports (Dehouck et al., 1995; Cecchelli et al., 1999). Ringer-HEPES (150 mM NaCl, 5.2 mM KCl, 2.2 mM $CaCl_2$, 0.2 mM $MgCl_2$, 6 mM $NaHCO_3$, 2.8 mM glucose, 5 mM HEPES) was added to the lower compartments of 12-well plate (2.3 ml per well), i.e. the abluminal side. One milliliter of Ringer-HEPES solution containing ^{14}C-labeled sucrose (1 μCi) with or without 200 μg/ml CBSA-NP was placed in the upper compartment at time 0, i.e. the luminal side. The incubations were performed on a rocking platform at 37 °C. At time 5, 10, 20, 30 and 60 min, the insert was transferred to another well of 12-well plate. An aliquot of 20 μl from each lower compartment and 10 μl from the initial solution containing ^{14}C-labeled sucrose in the upper compartment were dissolved in 3.0 ml of scintillation cocktail, respectively, and analyzed in a liquid scintillation counter (LKB1210, Wallac liquid scintillation, Sweden). The inserts only incubated with astrocytes for 12 days were used as control. Triplicate samples were performed.

Diffusion of sucrose across the BBB model was expressed in clearance terms according to the method of Siflinger-Birnboim et al. (1987) by dividing the cumulated amount of ^{14}C-labeled sucrose recovered in the abluminal side by its initial concentration in the luminal side. The mean cumulated cleared volumes were plotted versus time, which gave a linear relationship for the coculture model. The slope of the curve calculated by linear regression analysis corresponded to the clearance (μl/min) denoted PS_t, where PS was the permeability × surface area product. The slope of the clearance curve with the control filter only with the astrocytes on the bottom side was denoted PS_{as+f}. The PS value for the endothelial monolayer (PS_e) was calculated from:

$$\frac{1}{PS_e} = \frac{1}{PS_t} - \frac{1}{PS_{as+f}}$$

The PS_e values were divided by the surface area of the porous membrane (in this experiment was 0.9 cm^2) to generate the endothelial permeability coefficient (P_e, cm/min).

2.6. Uptake and transcytosis of 6-coumarin loaded CBSA-NP and BSA-NP in vitro

For the uptake study, BCECs were seeded at a density of 1×10^5 cells/cm^2 in 24-well plates. After 3–4 days, the medium was replaced with 1 ml 100 μg/ml suspension of nanoparticles in HBSS per well and the plate was incubated at 37 °C for 15, 30 min, 1, 2 and 4 h. At the end of each incubation period, the cells were washed with ice-cold uptake buffer, then with acid buffer at 4 °C for 5 min (consisting of 120 mM NaCl, 20 mM sodium barbital and 20 mM sodium acetate, pH 3) to remove the electrostatically bound CBSA-NP, and washed again with ice-cold uptake buffer (Thöle et al., 2002). Subsequently, the cells were solubilized in 400 μl 1% triton-X 100 and 20 μl of cell lysate from each well was used to determine the total cell protein content using BCA protein assay (Shenergy Biocolor Bioscience and Technology Co., Ltd., Shanghai, China). The remained lysates were lyophilized using ALPHA 2–4 Freeze Dryer (0.070 Mbar Vakuum, −80 °C, Martin Christ, Germany) for HPLC analysis of 6-coumarin (Davda and Labhasetwar, 2002; Panyam et al., 2003b). The uptake of nanoparticles by BCECs was calculated from the standard curve and expressed as the amount of nanoparticles (μg) taken up per mg cell protein.

The experimental procedure of transendothelial transport of 6-coumarin loaded nanoparticles through the coculture was the same as that of BBB permeability studies of ^{14}C-labeled sucrose above. One milliliter of 10 μg/ml 6-coumarin loaded CBSA-NP or BSA-NP in Ringer-HEPES solution was added to the luminal compartment, respectively. For the inhibition experiment, 1 mg/ml CBSA was additionally added to the 10 μg/ml 6-coumarin loaded CBSA-NP solution. At time 15, 30, 45 and 60 min after beginning, the insert was transferred to another well. The aluminal samples in each well (2.3 ml) were collected, lyophilized and analyzed by HPLC method. The inserts only incubated with astrocytes were used for control. Triplicate samples were performed. The data analysis of P_e was described above.

Table 1
The particle size and zeta potential of NPs and CBSA-NPs loaded or not with 6-coumarin ($n = 3$)

Nanoparticles	Mean size (mean ± SD, nm)	Size range (nm)	Zeta potential (mV)[a]
NP	83.5 ± 3.5	48.2–115.8	−9.36 ± 0.84
CBSA-NP	84.4 ± 3.0	75.9–100.1	−8.92 ± 0.65
6-coumarin loaded NP	80.4 ± 6.6	60.9–100.3	−16.81 ± 1.05
6-coumarin loaded CBSA-NP	82.1 ± 4.0	68.8–95.1	−12.19 ± 1.21
6-coumarin loaded BSA-NP	83.2 ± 43.6	70.4–96.8	−16.7 ± 0.86

[a] Measured in NaCl solution (1 mM).

2.7. Cytotoxicity of CBSA-NP against BCECs

The determination of cell viability is a common assay to evaluate the cytotoxicity of CBSA-NP by the MTT assays in vitro (Huang et al., 2004). BCECs were seeded onto 96-well plates at a density of 1×10^4 cells/well and cultured in 100 μl of cell growth medium for 2 days. The CBSA, NP and CBSA-NP samples were given a concentration of 0.025 to 8.0 mg/ml in HBSS. The resultant solutions were measured using an ELX800 Universal Microplate Reader (BIO-TEK Instruments Inc., USA) at λ_{570} test wavelength and λ_{630} reference wavelength. Cell viability was expressed as percentage of absorbance in comparison with that of the control, which comprised the cells only with HBSS. The experiments were performed in triplicates. The IC_{50} and IC_{20} represented the respective concentrations at which 50 and 20% of cell growth were inhibited.

3. Results

3.1. Characterization of nanoparticles

The number-based average diameters of NPs and CBSA-NPs loaded with or not with 6-coumarin were all in the range of 80–90 nm. There was no significant difference of particle size between nanoparticles conjugated with or without CBSA and loaded with or not with 6-coumarin, suggesting that neither the conjugation process with CBSA nor incorporation of the fluorescent dye influenced the particle size. The zeta potential values of the nanoparticles were all at the range of −8 to −17 mV, indicating that the CBSA did not cause dramatic inverse of the zeta potential (Table 1). The DLE of 6-coumarin loaded CBSA-NP and BSA-NP was 0.039 ± 0.003% and 0.038 ± 0.004%, respectively. However, such amount of dye was proved enough to be detected quantitatively in the in vitro cell uptake experiments (Davda and Labhasetwar, 2002; Panyam et al., 2003b). The CBSA-NP loaded with 6-coumarin was characterized by the leaching of dye under different 0.1 M PBS conditions (pH 4.0 and 7.4). Approximately 0.48% of the dye was released from the CBSA-NP in pH 4.0 compared with about 0.72% released in pH 7.4 in 72 h when the sinking condition was assured (Fig. 1).

3.2. Rat BCECs and astrocytes characterization

3.2.1. BCECs

The isolated majorities from newborn rat brain cortices examined under the microscope were the capillaries. We chose the way of cloning endothelial cell islands emerging from capillaries plated in vitro (Méresse et al., 1989; Gaillard et al., 2001). The capillaries were seeded into dishes coated with 1% gelatin, allowed to adhere. The first BCEC migrated out of the capillaries to form colonies 5 days after seed-

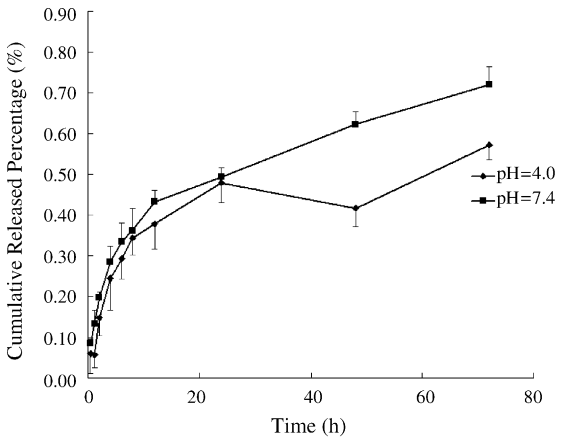

Fig. 1. In vitro release of 6-coumarin from CBSA-NP in 0.1MPBS buffer of pH 7.4 (square symbols) and 4.0 (diamond symbols).

ing. The colonies were sufficiently large 10 days after seeding, and the cells were characterized as cobblestone appearance. The five largest islands were trypsinized and seeded into another 35 mm diameter gelatin coated dish. BCECs reached confluency 5–6 days after passage (Fig. 2A). When confluent, BCECs presented a small, tightly packed, nonoverlapping, contact-inhibited and polygonal shape, forming a monolayer. BCECs were characterized by Factor VIII and the cell purity was more than 95%, indicating that it was pure enough to make the couture and nanoparticulate uptake experiment.

3.2.2. Astrocytes

According to our experience, the density of seeding cells must be high at the level above 1×10^6 cells/ml. The cells reached confluence 3 days after seeding. After 9–10 days, the cells stratified and the astrocytes formed the clusters in the bed layer. The shaking procedure of the astrocytes could guarantee the purity for our experiment request. It could effectively separate the astrocytes from microglias and oligodendrocytes' contaminations dominated on the upper layer. In this way, the purer astrocytes were harvested. The astrocytes reached confluence 2–3 days after shaking, and were subpassaged into the cell culture insert. Immunocytochemistry of glial fibrillary acidic protein (GFAP) result proved the purity of astrocytes to be more than 95%. Fischer and Kissel, 2001 said that astrocytes of the gray matter displayed small cell bodies with a few, short, highly branched cytoplasmatic processes; in contrast, astrocytes of the white matter were characterized by many long, but poorly ramified processes. These two types of astrocyte morphology were both found under SEM (Fig. 2B).

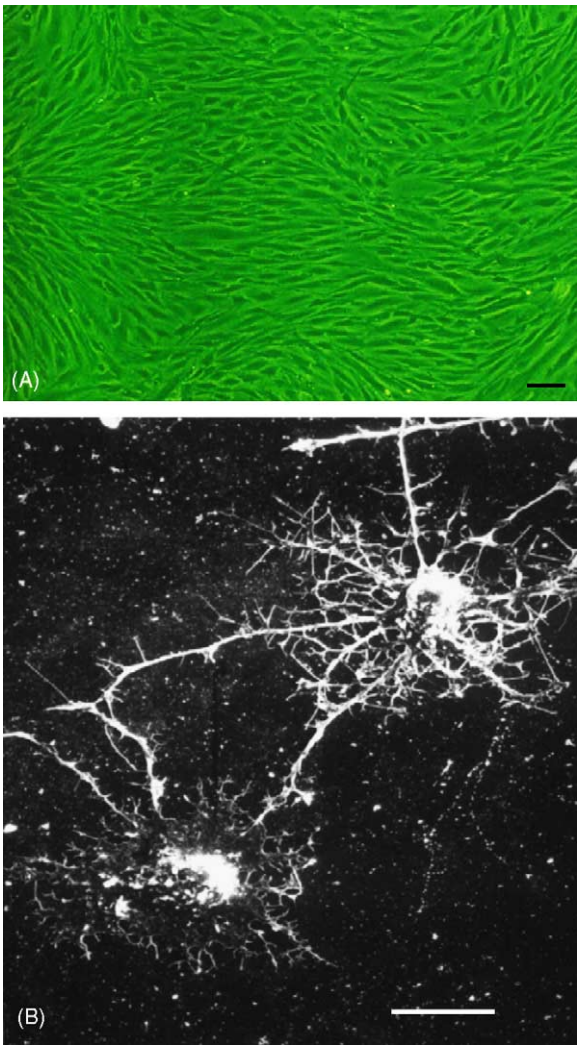

Fig. 2. Five days after passage of the colonies formed in the primary culture, BCECs reached confluence to form a monolayer of small, tight packed, nonoverlapping, contact-inhibited cells (A), bar is 100 μm. Scanning electron micrograph of astrocytes (B): protoplasmic astrocyte (left cell), dominated in the grey matter displayed small cell bodies with a few, short, highly branched cytoplasmatic processes; fibrous astrocyte (right cell), dominated in the white matter which were characterized by many long, but poorly ramified processes, bar is 15 μm.

3.3. Characterization of coculture of BCECs and astrocytes on the micro-porous membrane

The astrocytes reached confluence on the bottom side of PET membrane at day 4–5 (Fig. 3A), and only cell bodies could be visualized clearly as the light was not completely transmitted. BCECs reached confluence 4–5 days after seeding (Fig. 3B), and presented spindle or polygonal shape. After 10–12 days, tight junction was formed between BCECs. It was observed that the astrocytes proceeded their feet through the membrane pores to touch the upper BCECs from the bottom side under TEM (Fig. 3C). A close membrane apposition between two BCECs proved to be tight junction. Observation of coculture under SEM also showed a flat continuous non-overlapping monolayer of high compacted endothelial cells presenting narrow contacts

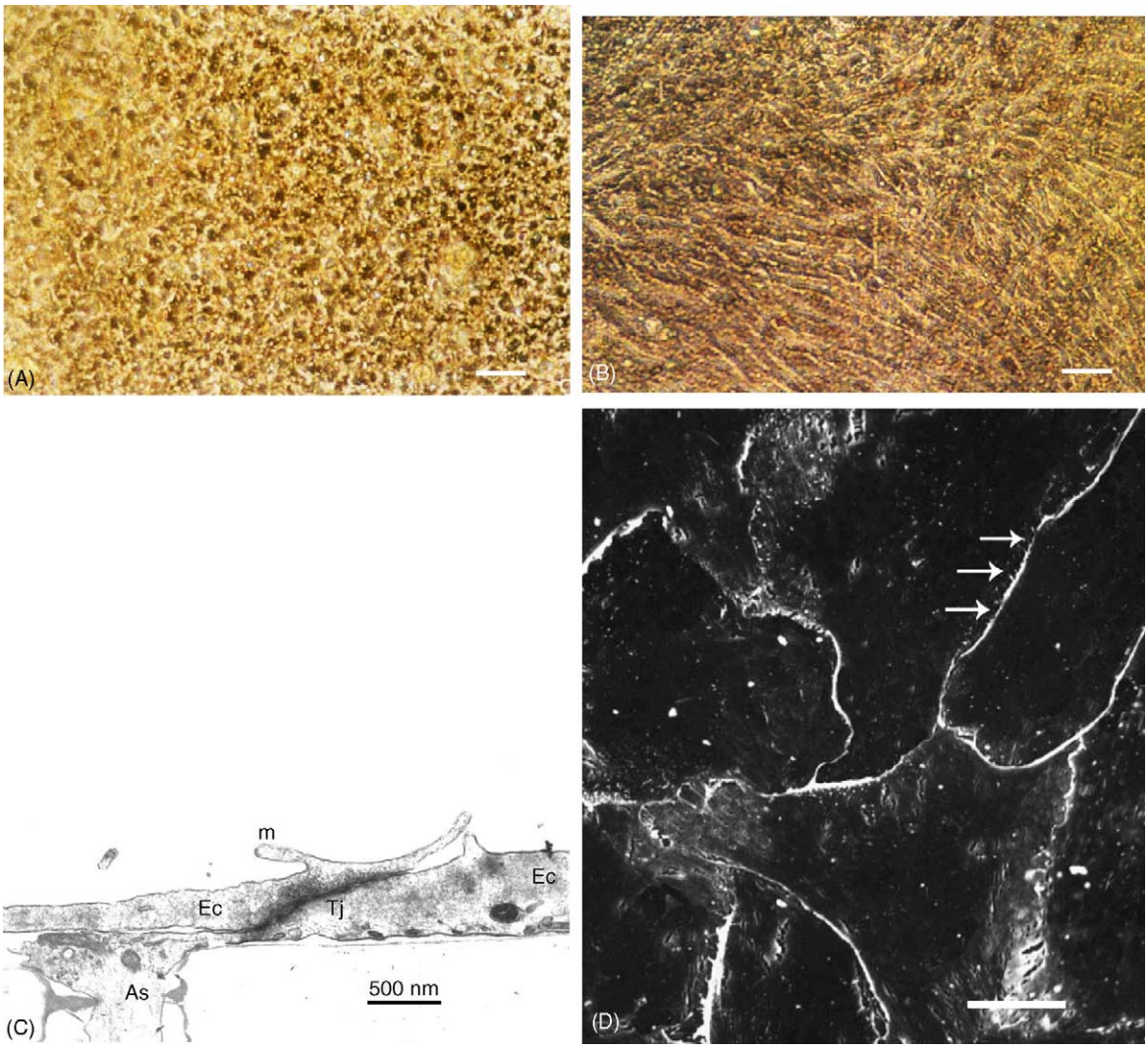

Fig. 3. Phase contrast micrograph of confluent astrocytes on the bottom side (A) and BCECs monolayer on the upper side (B) of the PET membrane 4–5 days after seeding, bars are both 50 μm. Transmission electron micrograph demonstrated an astrocyte endfoot (As) making contact with BCEC through a 1.0 μm diameter pore of PET membrane. A close membrane apposition represented tight junction (Tj) between two BCECs (Ec). "m" represents microvilli (C). Scanning electron micrograph also showed the tight junctions (arrows) between two endothelial cells of the BCEC monolayer onside of the micro-porous membrane of coculture (D), bar is 20 μm.

and tight junctions (Fig. 3D). TEER value of the coculture was detected as $313 \pm 23\ \Omega\ cm^2$.

3.4. Transendothelial transport study of ^{14}C-labeled sucrose

PS_t was attributed to the coculture including the BCEC monolayer, filter and astrocytes layer, while PS_{as+f} was ascribed to the filter and astrocytes as the control. PS_e calculated from PS_t and PS_{as+f} represented the PS of BCECs monolayer only, i.e. BBB in vitro. P_e of ^{14}C-labeled sucrose without and with 200 μg/ml CBSA-NP was 0.96×10^{-3} and 1.09×10^{-3} cm/min, respectively (Fig. 4). There was no significant difference of P_e value between ^{14}C-labeled sucrose with and without 200 μg/ml CBSA-NP. Since this concentration

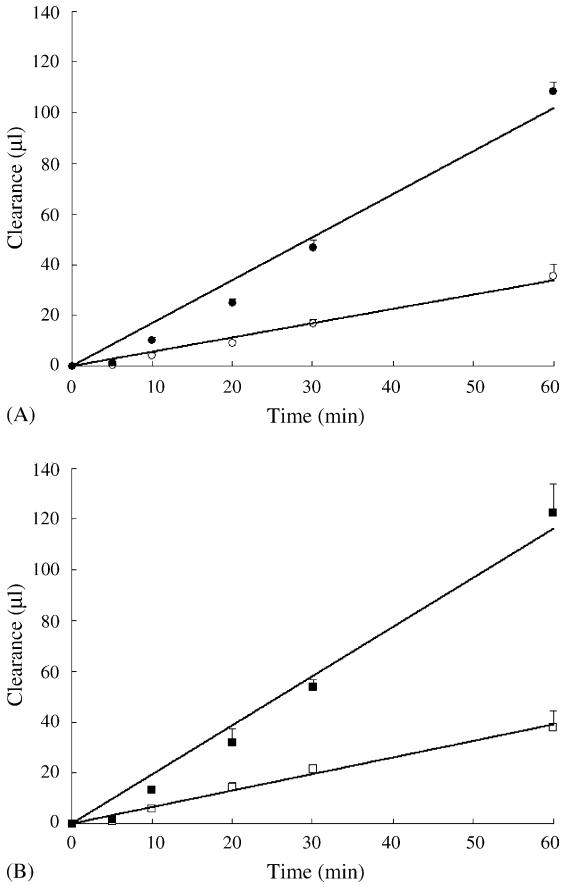

Fig. 4. (A) Clearance of ^{14}C-labeled sucrose across coculture model (circle and opened symbols) and cell culture insert only with the astrocytes layer (circle and closed symbols); (B) clearance of ^{14}C-labeled sucrose in appearance of 200 μg/ml CBSA-NP across coculture model (square and opened symbols) and cell culture insert only with the astrocytes layer (square and closed symbols); $n = 3$.

was believed that a dose significantly higher than would be presented to BBB with physiologic concentrations required in clinical therapy (Lockman et al., 2003), the 200 μg/ml CBSA-NP did not impact on the BBB tight junction in vitro.

3.5. Uptake and transendothelial transport study of 6-coumarin loaded nanoparticles

The uptake of CBSA-NP and BSA-NP by BCECs was dependent on the incubation time within 4 h (Fig. 5). At each time point, the uptake amount of the CBSA-NP was higher than that of BSA-NP, even

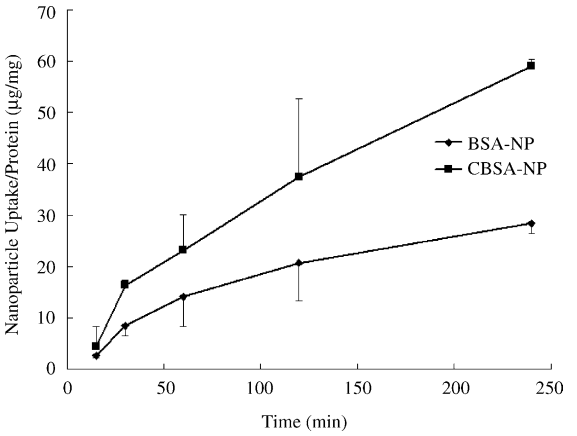

Fig. 5. BCECs uptake 100 μg/ml CBSA-NP (square symbols) and BSA-NP (diamond symbols) at 37 °C incubation for different time, respectively.

about two times higher than that of BSA-NP at 2 and 4 h.

Transendothelial transport of 10 μg/ml 6-coumarin loaded CBSA-NP (Fig. 6A) and BSA-NP (Fig. 6C) was determined in coculture, respectively, and the CBSA inhibition on the permeability of CBSA-NP was also performed (Fig. 6B). The membrane with 1 μm pore size was chosen to allow for free passage of the nanoparticles across the cell-free filters. P_e value of 6-coumarin loaded CBSA-NP was showed to be 7.76 times higher than that of 6-coumarin loaded BSA-NP; while 1 mg/ml CBSA can completely inhibit the permeability of 6-coumarin loaded CBSA-NP with its P_e value of 0.57 times than that of 6-coumarin loaded BSA-NP (Table 2). These results illustrated the significant transcytosis of CBSA-NP rather than BSA-NP in the BBB in vitro, which can be inhibited by free excessive CBSA.

3.6. Cytotoxicity of CBSA-NP against BCECs

MTT assay on BECEs viability showed that the cytotoxicity of CBSA, NP and CBSA-NP depended on their concentration ranging from 0.025 to 8 mg/ml (Fig. 7). From the viability–concentration curves, it can be derived that the IC_{20} of CBSA, NP and CBSA-NP was about 0.1, 1.5 and 1 mg/ml, and IC_{50} was 1, 5.9 and 4.8 mg/ml, respectively. There was no significant difference between NP and CBSA-NP.

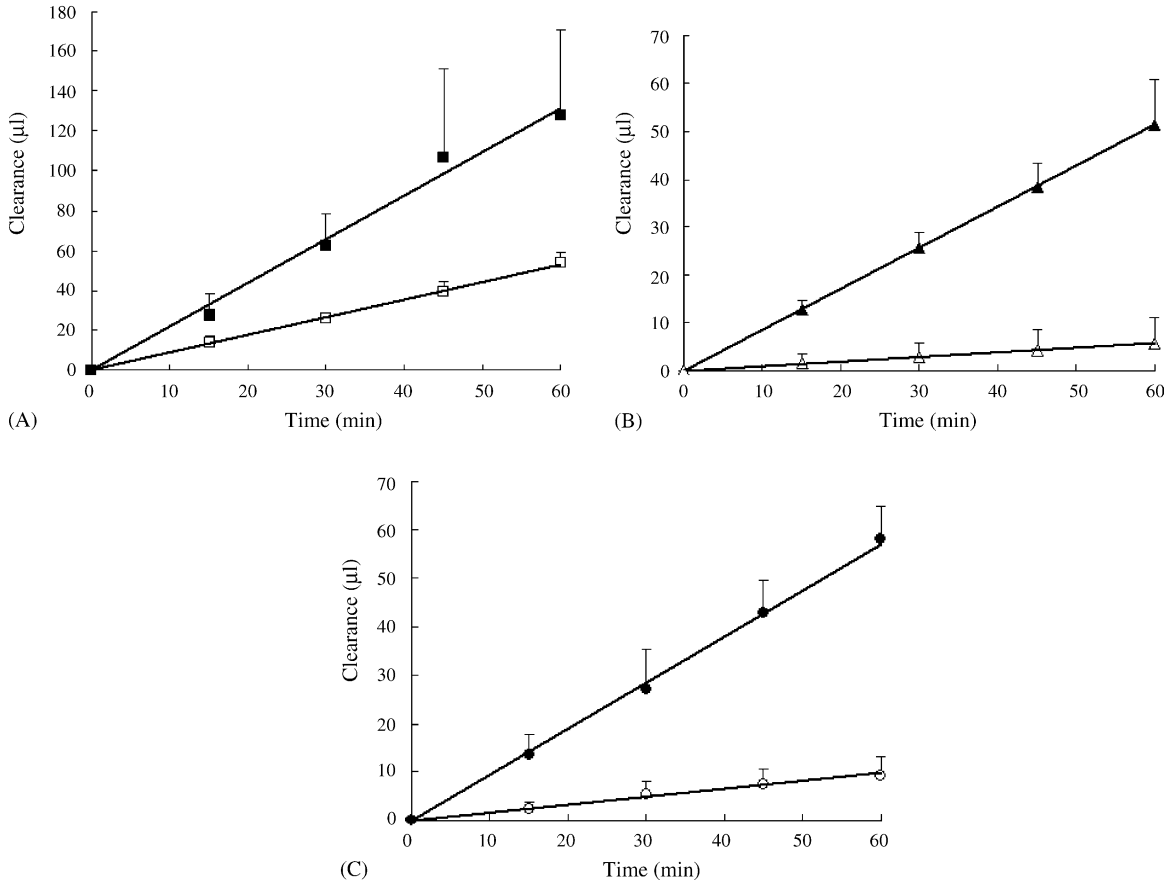

Fig. 6. The apparent PS of 10 μg/ml of CBSA-NP (A), CBSA-NP with 1 mg/ml free CBSA (B) and 10 μg/ml of BSA-NP (C) of rat BBB in vitro. Coculture model (opened symbols) and cell culture insert only with the astrocytes layer (closed symbols); $n = 3$.

4. Discussion

Our novel drug carrier of CBSA-NP was designed for the brain delivery. Its enhancement of brain uptake has been proven that the uptake amount of 6-coumarin loaded CBSA-NP by rat BCECs was much more than that of BSA-NP at 37 °C at different time incubation. This could be attributed to CBSA around the nanopaticle's surface. As the brain targetor, the free CBSA has been shown previously to permeate across the BBB through AMT process (Bickel et al., 2001). The investigation using isolated brain capillaries and evaluation with internal carotid perfusion/capillary depletion technique in vivo indicated a good accumulation profile of

Table 2
The apparent permeabilities (P_e) of BSA-NP and CBSA-NP of rat BBB in vitro ($n = 3$)

Nanoparticle concentration (10 μg/ml)	PS_t ($\times 10^{-3}$ ml/min)	PS_{as+f} ($\times 10^{-3}$ ml/min)	PS_e ($\times 10^{-3}$ ml/min)	P_e ($\times 10^{-3}$ cm/min)	P_e ratio of CBSA-NP to BSA-NP
CBSA-NP	0.88	2.19	1.47	1.63	7.76
CBSA-NP and CBSA	0.095	0.86	0.11	0.12	0.57
BSA-NP	0.16	0.95	0.19	0.21	–

CBSA concentration was 1 mg/ml.

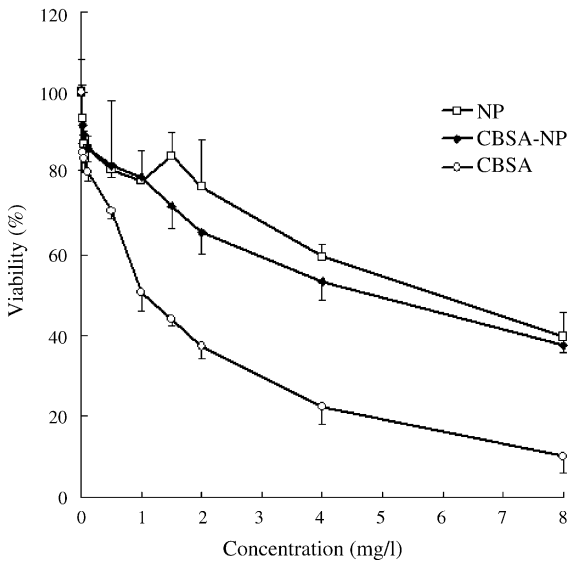

Fig. 7. In vitro cytotoxicity of NP (square and opened symbols), CBSA-NP (diamond and closed symbols) and CBSA (circle and opened symbols) on BCECs at concentration ranging from 0.025 to 8 mg/ml.

CBSA in the brain (Kumagai et al., 1987). Both apparent brain homogenate and postvascular supernatant volume of distribution of CBSA were much higher than BSA during a 10 min constant rate brain perfusion in rats (Triguero et al., 1990). The AMT mechanism has also been clarified in the CBSA coupled pegylated liposomes during the endothelial cell uptake process with caveolin-associated (Thöle et al., 2002). Therefore, the question was raised whether CBSA-NP with an average size range of 80–90 nm followed the same pathway.

To solve this problem, an in vitro BBB model was established to study its transcytosis ability. In order to undertake to further mimic the properties of BBB, we cultured the endothelial cells on the top side of the membrane of cell culture inserts and the astrocytes on the bottom side, which the astrocytes can spread their processes through the membrane pores to contact endothelial cells. In this pattern, it can realize the cell–cell interaction called "contact through feet" model (Hayashi et al., 1997). Since more and more evidence illustrated that astrocytes played an important role in the anatomical formation of BBB and functional expression of its specific properties (Hayashi et al., 1997; Isobe et al., 1996), this model can express specific functional proteins such as enzymes, transporters, tight junctional proteins, and reach higher TEER (Abbott, 2002; Demeuse et al., 2002). Evidence confirmed that the primary or low passage (under passage 7) brain capillary endothelial cells provided the closest phenotypic resemblance to the in vivo cell, and the cultured monolayers derived from them generated a restrictive paracellular barrier to solute permeability (Gumbleton and Audus, 2001; Cecchelli et al., 1999). We chose the coculture of rat BCECs associated with rat astrocytes to eliminate some disadvantages of cells originated from heterogeneous species (Demeuse et al., 2002). Considering the optimization of the coculture establishment, Demeuse et al. (2002) reported that the pore size optimized to be 1.0 μm allowed astrocytes to spread its feet through the membrane while the whole cell body was not able to migrate. Smaller pore size such as 0.4 μm did not permit the astrocyte's endfeet to reach the opposite side of the membrane through these pores. A larger pore size (3.0 μm) could induce astrocytes migration. The polycarbonate membrane was not transparent under the optical reversed phase contrast microscope so that we cannot visualize the cell growth. The PET membrane chosen here seemed to be fairly suitable for endothelial cells growth, and it was easy to be visualized under light microscope. The cell morphology and growth rate on PET membrane were similar to that on the plastic dish.

Tight junctions between the brain capillary endothelial cells played an important role in maintaining the barrier properties of the BBB in vivo. The characterization results of the coculture showed that it made TEER values 313 $\Omega\,cm^2$ which was in the range of 300–1000 $\Omega\,cm^2$ of BBB in vitro model (Demeuse et al., 2002). TEM displayed the tight junction between two endothelial cells and the astrocyte can spread its foot through the membrane pore to touch the endothelial cells. SEM also showed this flat, continuous and non-overlapping monolayer of highly compacted BCECs onside of the micro-porous membrane. As a matter of fact, our coculture was "tight enough" and suitable for the investigation of drug or nanoparticulate transport through BBB.

As several in vitro BBB models were used to determine the effect of nanoparticles or immunoliposomes on the permeability changing of the paracellular transport marker such as inulin and sucrose (Lockman et al., 2003; Olivier et al., 1999; Kreuter et al., 2003; Cerletti et al., 2000), the tight junction seemed most impor-

tant for evaluation of the impact of these drug carriers on BBB integrity. The permeability coefficient of sucrose calculated herein (0.96×10^{-3} cm/min) agreed with previously published data (0.75×10^{-3} cm/min), which was smaller than that of BCEC monolayer without astrocyte coculture (1.9×10^{-3} cm/min) (Cecchelli et al., 1999; Dehouck et al., 1995). This value ensured that our coculture model was reliable. Given that there was no significant difference between the sucrose P_e value with and without CBSA-NP, we suggested that the CBSA-NP solutions with its concentration lower than 200 μg/ml have no effect on the BCEC tight junction integrity during the 60 min transport experiment.

In vitro transcytosis result of CBSA-NP demonstrated that CBSA-NP preferentially crossed the brain capillary endothelium. Transendothelial transport of CBSA-NP showed the P_e value was about 7.76 times higher than that of BSA-NP. This transport was mediated by CBSA because little transcytosis was observed by competition with an excess of free CBSA. The MTT assay on BECEs viability showed that the cytotoxicity of CBSA-NP (IC_{20} and IC_{50}) was likely to CBSA unconjugated pegylated nanoparticles (NP), which seemed much less toxic since they were shown to have an acceptable safety profile in rats (Plard and Bazile, 1999). The result of insignificant change of the sucrose permeability in coculture model was in consistence with MTT assay, suggesting that the brain entry pathway of CBSA-NP was due to transcytosis instead of intercellular leakage. Thus, we can conclude that the AMT process was involved in the CBSA-NP transport across BBB.

We, for the first time, applied the fluorescent dye to detect the nanoparticle for the in vitro permeability study. Previous report showed that about 0.10% of the encapsulated 6-coumarin was released from poly(D,L-lactide-co-glycolide) (PLGA) nanoparticles in PBS with pH 4 and about 0.45% released in PBS with pH 7.4 in 48 h (Panyam et al., 2003b). Our in vitro release test also confirmed this characteristic. The relative inertia of 6-coumarin encapsulated in CBSA-NP guaranteed that the dye was not released under the physiological condition or in the acidic endo-lysosome compartment (Panyam et al., 2003b), which ensured 6-coumarin to be an accurate probe for the nanoparticle's detection. Furthermore, the dye has also been used to investigate dynamics of endocytosis and exocytosis of PLGA nanoparticles in the vascular smooth muscle cells (Panyam and Labhasetwar, 2003a) and qualitative and quantitative analysis of uptake of PLGA nanoparticles by the human umbilical vein endothelial cell (Davda and Labhasetwar, 2002). Since the detection limit of the 6-coumarin was sensitive enough by using HPLC fluorescence detector (Davda and Labhasetwar, 2002; Panyam et al., 2003b), it was succeeded in our transcytosis experiment.

5. Conclusions

In this paper, we established a synergic coculture of rat BCECs and astrocytes with high paracellular resistance. This in vitro experimental model of the rat BBB was close enough to resemble the in vivo situation for examination of the permeability of CBSA-NP and toxicity evaluation. The unchanged paracellular transport of sucrose proved that CBSA-NP with its concentration lower than 200 μg/ml did not impact the integrity of BBB endothelial tight junctions. The P_e value of CBSA-NP was significantly higher than that of BSA-NP, while the transport was inhibited in the excess of free CBSA. We can conclude that CBSA-NP preferentially transported across BBB without opening the endothelial tight junction, which offered the possibility to deliver therapeutic agents to CNS.

Acknowledgements

This work was supported by National Natural Science Foundation of China (30472095), Nanotechnology Project of Shanghai Science and Technology Committee (0243nm067) and Innovation Foundation of Graduate Students of Fudan University. The authors acknowledge Dr. Jörg Huwyler, Dept. of Research and Clinical Pharmacology, University Hospital, CH-4031 Basel, Switzerland, for the discussion with the transendothelial transport study in BBB in vitro model, and thank for his best advice on the transcytosis experiment design.

References

Abbott, N.J., 2002. Astrocyte-endothelial interactions and blood–brain barrier permeability. J. Anat. 200, 629–638.

Bazile, D., Prud'homme, C., Bassoullet, M.T., Marlard, M., Spenlehauer, G., Veillard, M., 1995. Stealth Me.PEG-PLA nanoparticles avoid uptake by the mononuclear phagocyte system. J. Pharm. Sci. 84, 493–498.

Bickel, U., Yoshikawa, T., Pardridge, W.M., 2001. Delivery of peptides and proteins through the blood–brain barrier. Adv. Drug Deliv. Rev. 46, 247–279.

Cecchelli, R., Dehouck, B., Descamps, L., Fenart, L., Buée-Scherrer, V., Duhem, C., Lundquist, S., Rentfel, M., Torpier, G., Dehouck, M.P., 1999. In vitro model for evaluating drug transport across the blood–brain barrier. Adv. Drug Del. Rev. 36, 165–178.

Cerletti, A., Drewe, J., Fricker, G., Eberle, A.N., Huwyler, J., 2000. Endocytosis and transcytosis of an immunoliposome-based brain drug delivery system. J. Drug Target. 8, 435–446.

Davda, J., Labhasetwar, V., 2002. Characterization of nanoparticle uptake by endothelial cells. Int. J. Pharm. 233, 51–59.

Dehouck, M.P., Dehouck, B., Schluep, C., Lemaire, M., Cecchelli, R., 1995. Drug transport to the brain: comparison between in vitro and in vivo models of the blood–brain barrier. Eur. J. Pharm. Sci. 3, 357–365.

Dehouck, M.P., Jolliet-Riant, P., Bree, F., Fruchart, J.C., Cecchelli, R., Tillement, J.P., 1992. Drug transfer across the blood–brain barrier: correlation between in vitro and in vivo models. J. Neurochem. 58, 1790–1797.

Demeuse, Ph., Kerkhofs, A., Struys-Ponsar, C., Knoops, B., Remacle, C., van den Bosch de Aguilar, Ph., 2002. Compartmentalized coculture of rat brain endothelial cells and astrocytes: a syngenic model to study the blood–brain barrier. J. Neurosci. Meth. 121, 21–31.

Ellmann, G.L., 1959. Tissue sulfhydryl groups. Arch. Biochem. Biophys. 82, 70–77.

Fischer, D., Kissel, T., 2001. Histochemical characterization of primary capillary endothelial cells from porcine brains using monoclonal antibodies and fluorescein isothiocyanate-labelled lectins: implications for drug delivery. Eur. J. Pharm. Biopharm. 52, 1–11.

Gaillard, P.J., Voorwinden, L.H., Nielsen, J.L., Ivanov, A., Atsumi, R., Engman, H., Ringbom, C., de Boer, A.G., Breimer, D.D., 2001. Establishment and functional characterization of an in vitro model of the blood–brain barrier, comprising a co-culture of brain capillary endothelial cells and astrocytes. Eur. J. Pharm. Sci. 12, 215–222.

Gumbleton, M., Audus, K.L., 2001. Progress and limitations in the use of in vitro cell cultures to serve as a permeability screen for the blood–brain barrier. J. Pharm. Sci. 90, 1681–1698.

Hayashi, Y., Nomura, M., Yamagishi, S.I., Harada, S.I., Yamashita, J., Yamamoto, H., 1997. Induction of various blood–brain barrier properties in non-neural endothelial cells by close apposition to co-cultured astrocytes. Glia 19, 13–26.

Huang, M., Khor, E., Lim, L.Y., 2004. Uptake and cytotoxicity of chitosan molecules and nanoparticles: effects of molecular weight and degree of deacetylation. Pharm. Res. 21, 344–353.

Huwyler, J., Wu, D., Pardridge, W.M., 1996. Brain drug delivery of small molecules using immunoliposomes. Proc. Natl. Acad. Sci. U.S.A. 93, 14164–14169.

Isobe, I., Watanabe, T., Yotsuyanagi, T., Hazemoto, N., Yamagata, K., Ueki, T., Nakanishi, K., Asai, K., Kato, T., 1996. Astrocytic contributions to blood–brain barrier (BBB) formation by endothelial cells: a possible use of aortic endothelial cell for in vitro BBB model. Neurochem. Int. 28, 523–533.

Kreuter, J., Ramge, P., Petrov, V., Hamm, S., Gelperina, S.E., Engelhardt, B., Alyautdin, R., von Briesen, H., Begley, D.J., 2003. Direct evidence that polysorbate-80-coated poly(butylcyanoacrylate) nanoparticles deliver drugs to the CNS via specific mechanisms requiring prior binding of drug to the nanoparticles. Pharm. Res. 20, 409–416.

Kumagai, A.K., Eisenberg, J., Pardridge, W.M., 1987. Absorptive-mediated endocytosis of cationized albumin and a b-endorphin-cationized albumin chimeric peptide by isolated brain capillaries. Model system of blood–brain barrier transport. J. Biol. Chem. 262, 15214–15219.

Lockman, P.R., Koziara, J., Roder, K.E., Paulson, J., Abbruscato, T.J., Mumper, R.J., Allen, D.D., 2003. In vivo and in vitro assessment of baseline blood–brain barrier parameters in the presence of novel nanoparticles. Pharm. Res. 20, 705–713.

McCarthy, K.D., De Vellis, J., 1980. Preparation of separate astroglial and oligodendroglial cell cultures from rat cerebral tissue. J. Cell. Biol. 85, 890–902.

Méresse, S., Dehouck, M.P., Delorme, P., Bensaid, M., Tauber, J.P., Delbart, C., Fruchart, J.C., Cecchelli, R., 1989. Bovine brain endothelial cells express tight junctions and monoamine oxidase activity in long-term culture. J. Neurochem. 53, 1363–1371.

Olivier, J.C., Fenart, L., Chauvet, R., Pariat, C., Cecchelli, R., Couet, W., 1999. Indirect evidence that drug brain targeting using polysorbate 80-coated polybutylcyanoacrylate nanoparticles is related to toxicity. Pharm. Res. 16, 1836–1842.

Olivier, J.C., Huertas, R., Lee, H.J., Calon, F., Pardridge, W.M., 2002. Synthesis of pegylated immunonanoparticles. Pharm. Res. 19, 1137–1143.

Panyam, J., Labhasetwar, V., 2003a. Dynamics of endocytosis and exocytosis of poly(D,L-lactide-co-glycolide) nanoparticles in vascular smooth muscle cells. Pharm. Res. 20, 212–220.

Panyam, J., Sahoo, S.K., Prabha, S., Bargar, T., Labhasetwar, V., 2003b. Fluorescence and electron microscopy probes for cellular and tissue uptake of poly(D,L-lactide-co-glycolide) nanoparticles. Int. J. Pharm. 262, 1–11.

Pardridge, W.M., 2003. Blood–brain barrier drug targeting: the future of brain drug development. Mol. Intervent. 3, 90–105.

Plard, J.P., Bazile, D., 1999. Comparison of the safety profiles of PLA_{50} and Me.PEG-PLA_{50} nanoparticles after single dose intravenous administration to rats. Colloids Surf. B: Biointerf. 16, 173–183.

Shi, N., Pardridge, W.M., 2000. Noninvasive gene targeting to the brain. Proc. Natl. Acad. Sci. U.S.A. 97, 7567–7572.

Shi, N., Zhang, Y., Zhu, C., Boado, R.J., Pardridge, W.M., 2001. Brain-specific expression of an exogenous gene after i.v. administration. Proc. Natl. Acad. Sci. U.S.A. 98, 12754–12759.

Siflinger-Birnboim, A., Del Becchio, P.J., Cooper, J.A., Blumenstock, F.A., Shepard, J.N., Malik, A.B., 1987. Molecular sieving characteristics of the cultured endothelial monolayer. J. Cell. Physiol. 132, 111–117.

Thöle, M., Nobmann, S., Huwyler, J., Bartmann, A., Fricker, G., 2002. Uptake of cationized albumin coupled liposomes by cul-

tured porcine brain microvessel endothelial cells and intact brain capillaries. J. Drug Target. 10, 337–344.

Triguero, D., Buciak, J.B., Pardridge, W.M., 1990. Capillary depletion method for quantifying blood–brain barrier transcytosis of circulating peptides and plasma proteins. J. Neurochem. 54, 1882–1888.

Zhang, Y., Calon, F., Zhu, C., Boado, R.J., Pardridge, W.M., 2003. Intravenous nonviral gene therapy causes normalization of striatal tyrosine hydroxylase and reversal of motor impairment in experimental parkinsonism. Human Gene Ther. 14, 1–12.

Zhang, Y., Schlachetzki, F., Zhang, Y.F., Boado, R.J., Pardridge, W.M., 2004. Normalization of striatal tyrosine hydroxylase and reversal of motor impairment in experimental parkinsonism with intravenous nonviral gene therapy and a brain-specific promoter. Human Gene Ther. 15, 339–350.